ISSN:
Print - 2277 - 0593
Online - 2315 - 7461
© FUNAAB 2022

Journal of Natural Science, Engineering and Technology

ARTIFICIAL NEURAL NETWORK MODELLING OF ABOVEGROUND BIOMASS FROM TROPICAL RAIN FORESTS IN NIGERIA

***[1]S. J. OKONKWO AND [2]Z. H. MSHELIA**

*Department of Environmental Modelling and Biometrics
Forestry Research Institute of Nigeria, Forest Hill, Jericho, Ibadan
***Corresponding Author:** sj.okonkwo@gmail.com **Tel:** 08185940603

ABSTRACT

This study investigated the impact of applying artificial neural networks (ANNs) with different input variables and different architectures to estimate aboveground biomass (AGB) using allometric data from tropical forests in Southwestern Nigeria. The study also compared the result of ANNs with linear regression. Three fully connected feed-forward neural networks (all four-layer) with backpropagation of error were used in this study. They had two hidden layers: the first two had topography [2, 3, 3, 1], and the third had topography [3, 5, 5, 1]. Rectified Linear Unit (ReLU) activation function was used for all networks; Mean Squared Error (MSE) was used as the loss function. A learning rate of 1e-06 and 1000 iterations was used to run the first two ANNs, and a learning rate of 1e-06 and 1850 iterations was used to run the third. Maximum loss for each neural network was 12.8393, 12.0371, and 0.2078, respectively, while minimum loss was 0.0391, 0.0408, and 0.1559, respectively. Accuracy was measured using Root Mean Squared Error (RMSE) with the training for each neural network RMSE's being 0.1997, 0.2113 and 0.3949 while test RMSE's was 0.2199, 0.2284, and 0.3812 for each neural network.

Keywords: Aboveground Biomass, Neural Network, Regression, ReLU, RMSE

DOI:

INTRODUCTION

Forests play an important role in global carbon cycling because they act as carbon sinks and sources for atmospheric CO2 (Pan *et al.* 2011; Chave *et al.* 2014). Forest aboveground biomass (AGB) is an indicator for assessing forest ecosystem productivity and health as well as an indicator for determining the potential for carbon storage and carbon sink, as well as an important parameter for estimating carbon emissions and disturbances caused by land use and climate change (Baccini *et al.*, 2017 and Rodríguez-Soalleiro *et al.*, 2018). More accurate estimation of trees aboveground biomass (AGB) in forests is needed to determine commercial use of forest production, stand density, fuel and bio-energy contribution, and the role of forest biomass in the global carbon cycle. Currently, the most accurate methods for obtaining forest AGB are the use of the site- and species-specific allometric equations based on measured forest biometric parameters, such as the diameter at breast height

(DBH), height, crown closure, and stem density (Chave *et al.* 2014; Ali *et al.* 2015; Paul *et al.* 2015).

There are major concerns with selecting the best regression model to estimate tree AGB in natural forests. Stevens, (2009) declared that because many growth data empirically turned out to align along a straight line when plotted in log-transformed scales, power models have played a substantial role in allometry. In contrast, others opined that allometry should go beyond power-law models because the growth data do not exactly align along a straight line in log-log plots (Bernacci *et al.*, 2000 and Picard *et al.*, 2015). However, Sileshi, (2014) argued that some allometric equations are dubious due to lack of taking into consideration some validation indicators like collinearity among the predictors and reliability of parameters estimate.

To reexamine the issue of whether or not power-law models are the best predictors for biomass estimation, an artificial neural network (ANN) based system was used to be compared to a traditional allometric method (regression analysis). There has been a substantial increase in the interest in artificial neural networks (ANNs) during the last 15 years (Kumar *et al.*, 2015). Considering the complexity of relationships between the response and explanatory variables and of different views and major concerns associated with allometric equations application for prediction of trees AGB, ANN may be the best alternative to decrease the obscurity of biomass estimation.

MATERIALS AND METHODS

Data Collection

A Forest inventory-based approach was adopted to estimate above-ground tree biomass in the study areas. Transects were distributed over the entire forest, using a systematic segmented grid (Buckland *et al.*, 2004) randomly superimposed onto the area. There were 5111 plots of 30 × 30m in Omo Biosphere Reserve. The forest inventory was conducted in 50 plots of 30 × 30m sample plots which was 1% sample intensity. All the trees in each sample plot were labelled with the use of paper tape and markers to avoid leaving out any tree and also for easy identification. Data were also collected for model validation on 9 plots of 30 × 30 m in Akure Forest Reserve. Field measurements of tree variables were carried out using relascope, Haga altimeter, increment borer, scale weight, measuring tape, ranging pole, and Global Positioning System (GPS).

Determination of Biomass and Carbon Stock in the Study Area

Measurement of total height

This is the vertical distance between the ground level and the tip of a tree. It is obtained by taking the reading at the top (RT) and reading at the base (RB) which is usually negative (when on an elevated ground) and positive (when in a depressed ground or valley). It was measured with the aid of Spiegel Relaskop.

Total height (H), using the metric scale was obtained by:

$$H = RT\text{-}RB \quad \ldots\ldots\ldots\ldots\ldots\ldots\ldots\ldots(1)$$

Where is the height, is the reading at the top, and is the reading at the base.

Measurement of tree diameter at Breast height (DBH)

This is the diameter measurement taken for a standing tree at height 1.30 m above the ground level. This tree parameter was taken for trees within the permanent sample plots.

This measurement is generally accepted in forest inventory (Elzinga *et al.*, 2005). It is the easiest measurable parameter in forest inventory with high degree of accuracy where guiding rules are followed. It was measured with the aid of diameter tape in centimetres (cm).

Diameter at middle (Dm) and Diameter at the top (Dt) were also measured at various positions on the standing tree using Spiegel relaskop. Readings for Dm and Dt were taken in terms of numbers of bands of the relaskop occupied by the stem of the trees both at the middle and the top. These bands of relaskop are of two types: dark bands which are one unit each and big white bands which are four units each.

Wood Density

To determine the specific wood density, core samples were collected for each species at breast height. The specific wood density is the arithmetic average value of all samples of a species and were calculated as oven dry weight divided by fresh volume of each sample. The inner diameter of the bit of the increment borer device was 0.5 cm leading to a diameter of the sample of 0.5 cm. The length L of the sample was measured after its extraction. The oven dry density (ϱ) in terms of dry mass per fresh volume (g/cm^3) of all collected wood samples was estimated using

$$\rho = \frac{4dMSi}{\pi d^2 Li} \qquad \ldots\ldots\ldots (2)$$

Where $dMSi$ is the dry mass of wood sample i obtained by the increment borer, d is the diameter of the bit, and Li is the length of the sample i.

Data Processing and Analysis

Basal Area Estimation

Tree Basal Area (TBA) is the cross-sectional area (over the bark) at breast height (1.3 metres above the ground) measured in metres squared (m^2). The TBA can be used to estimate tree volumes and stand competition. The Tree Basal Area was determined by measuring the diameter at breast height in centimetres and the basal area (m^2) was calculated using an equation based on the formula for the area of a circle (area = πr^2 where r = radius and π = 3.142) and the formula for radius (r =diameter/2 = DBH/2).

$$BA(m^2) = \pi r^2 * DBH(cm)^2 /4 \qquad \ldots(3)$$

Volume Estimation

Volume for each tree was estimated using the Newton's formula

$$V = \pi H \left(\frac{Db^2 + 4Dm^2 + Dt^2}{24} \right) \qquad \ldots\ldots\ldots(4)$$

Where V is the stem volume (m^3), H is the total height (m), Db is the diameter at base (cm), Dm is the diameter at the middle (cm), and Dt is the Diameter at the top (cm).

Above-Ground Biomass (AGB) Calculation

The above ground biomass (AGB) for each tree was estimated using the formula:

$$AGB = V \times \rho \times B_{ef} \qquad \ldots\ldots\ldots(5)$$

Where AGB (t/ha) measured in tonne per hectare is the aboveground biomass of the tree, V is the volume of tree (m^3/ha) measured in cubic metre per hectare, ρ is the specific wood density (t/m^3), and B_{ef} is the biomass expansion factor.

Regression Model Development

Based on the data collected, three equations were developed. Prior to the establishing of the allometric equation, scatter plots were used to ascertain that the relationship between independent and dependent variables was linear. Furthermore, several allometric relationships between independent and dependent variables were tested. The independent variables included DBH (D), height (H) and wood density (W), whereas, the dependent variable was AGB (A).

$$\ln(A) = \alpha + \beta(DH) \quad \ldots\ldots(6)$$

$$\ln(A) = \alpha + \beta(D^2H) \quad \ldots\ldots(7)$$

$$\ln(A) = \alpha + \beta(D^2HW) \quad \ldots\ldots(8)$$

Where: ln is the natural logarithm; α is the intercept; β and is the slope.

Model Development for Artificial Neural Networks

Three fully connected feed forward neural networks (all four–layer) with backpropagation of error were used in this study. They had two hidden layers: the first two had topography 2, 3, 3, 1, and the third had topography 3, 5, 5, 1. Rectified Linear Unit (ReLU) activation function was used for all networks, and half of the Mean Squared Error (HMSE) was used as the loss function.

Let W_i and b_i be the vector of weights and biases for layer i of the neural network. The weights and biases for all layers of the neural networks were randomly initialized from a normal distribution with arbitrary minimum and maximum values.

Forward Propagation

Let Z_1 be the sum of the vector of biases for the first layer b_1 , and the dot product of the input vector X_{OAV} and the weight of the first layer W_1 such that:

$$Z_1 = b_1 + X_{OAV} \cdot W_1 \quad \ldots\ldots\ldots\ldots(9)$$

Let z be an element of Z_i for layer i, the input vector for layer i + 1 denoted by A_i is derived by the application of the activation function (Rectified Linear Unit or ReLU) (Fukushima, 1980; Nair & Hilton, 2010; and Schmidhbuer, 2014) on each element of Z_i such that:

$$A_i = ReLU(Z_i) \quad \ldots\ldots\ldots\ldots(10)$$

Where ReLU performs a threshold operation to each input element where values less than zero are set to zero, such that:

$$f(z) = \max(0, z) \quad \ldots\ldots(11)$$

Generalizing (11) above subsequently for layer i of the neural network, we have:

$$Z_i = b_i + A_{i-1} \cdot W_i \quad \ldots.(12)$$

The output vector of the neural network is given as:

$$\hat{Y}_{AGB} = ReLU(Z_f) \quad \ldots..(13)$$

Where $\hat{Y}_{AGB}$ is the vector of the predicted output variable; and Z_f is the sum of the bias vector and the dot product between the input vector and weight vector of the final layer.

Loss Function

The loss function used is the Mean Squared Error (MSE) and is defined as:

$$\text{MSE} = \frac{1}{n}\sum_{i=1}^{n}\left(Y_{AGB} - \hat{Y}_{AGB}\right)^2 \quad \ldots\ldots(14)$$

Back Propagation

Differentiating the Loss Function MSE in (14) with respect to $\hat{Y}_{AGB}$, results in:

$$\frac{\partial MSE}{\partial \hat{Y}_{AGB}} = \frac{2}{n}\sum_{i=1}^{n}\left(Y_{AGB} - \hat{Y}_{AGB}\right) \tag{15}$$

From (13) above, differentiating the output vector of the neural network $\hat{Y}_{AGB}$ with respect to Z_f is given by:

$$\frac{\partial \hat{Y}_{AGB}}{\partial Z_f} = \partial ReLU(Z_f) \tag{16}$$

Where $\partial ReLU(Z_f)$ is defined by

$$f(z) = \begin{cases} 0 \; if \; z < 0 \\ 1 \; if \; z > 0 \end{cases} \tag{17}$$

Differentiating the Loss Function MSE with respect to Z_f is given by:

$$\frac{\partial MSE}{\partial Z_f} = \frac{\partial MSE}{\partial \hat{Y}_{AGB}} \times \frac{\partial \hat{Y}_{AGB}}{\partial Z_f} \tag{18}$$

$$= \frac{2}{n}\sum_{i=1}^{n}\left(Y_{AGB} - \hat{Y}_{AGB}\right) \times \partial ReLU(Z_f)$$

From (12) above, differentiating Z_i with respect to Z_{i-1} is given by:

$$\frac{\partial Z_i}{\partial Z_{i-1}} = \frac{\partial Z_i}{\partial A_{i-1}} \times \frac{\partial A_{i-1}}{\partial Z_{i-1}} \tag{19}$$

$$= \frac{\partial Z_{i+1}}{\partial Z_i} \times \partial ReLU(Z_{i-1})$$

Differentiating Z_i in (12) with respect to W_i results in:

$$\frac{\partial Z_i}{\partial W_i} = {A_{i-1}}^{T} \cdot \frac{\partial A_i}{\partial Z_i} \tag{20}$$

Differentiating Z_i in (12) with respect to b_i results in:

$$\frac{\partial Z_i}{\partial b_i} = \sum_{j=1}^{n}\frac{\partial Z_i}{\partial W_i} \tag{21}$$

Let τ be the learning rate of the neural network. The vector of weight W_i and bias b_i for each layer i are updated by the following equations:

$$W_i = W_i - \tau * \frac{\partial Z_i}{\partial W_i} \tag{22}$$

$$b_i = b_i - \tau * \frac{\partial Z_i}{\partial b_i} \tag{23}$$

Accuracy

Accuracy was measured using Root Mean Square Error (RMSE) defined as:

$$RMSE = \sqrt{\frac{1}{n}\sum_{i=1}^{n}\left(Y_{AGB} - \hat{Y}_{AGB}\right)^2} \quad (24)$$

Analysis

Analysis was carried out using Python Programming Language version 3.8 (Van Rossum & Drake, 2009). Packages used include NumPy (Oliphant, 2006; van der Walt *et al.*, 2011), Matplotlib (Hunter, 2007), Pandas (McKinney & others, 2010), SciPy (Virtanen *et al.*, 2020), and Scikit-learn (Pedregosa *et al.*, 2011). Data were split into two parts: training set (80%) and validation set (20%).

Regression analysis was first carried out on the data, using the allometric models in equations 6, 7 and 8 above to estimate parameters α and β. The resulting estimated parameters were thereafter used to create regression models between the dependent variable (In (AGB)) and the independent variable (In(DH), In(D^2H), In(D^2HW)) of each allometric models. The input data from the validation set is then inputted in the regression model to predict $\widehat{ln\ (AGB)}$. For the ANN models, a learning rate of 1e-06 and 1000 iterations was used to run the first two ANNs, and a learning rate of 1e-06 and 1850 iterations was used to run the third. The predicted values for both the regression and ANN models were compared with the test values and accuracy was measured with Root Mean Square Error (RMSE).

RESULTS AND DISCUSSION

The output variable In(A) had a mean of 4.135 and a standard deviation of 0.679. It also had a strong correlation concerning all input variables used in this study. With a mean of 6.524 and standard deviation of 0.689, the first explanatory In(DH) variable had a covariance of 0.382041 and a correlation of 0.815684 with respect to the output variable In(A). In(D^2H) had a mean of 10.119 and standard deviation of 1.136, and it had a covariance of 0.624536 and correlation of 0.808669 concerning In(A). In (D^2HW) had a covariance of 0.629540 and correlation of 0.850021, with a mean of 9.605 and standard deviation of 1.089.

Table 1: Summary of Explanatory Variables and Regression Model Details

Explanatory Variable	Covariance	Correlation	Mean	Standard Deviation	Rsq	Intercept (α)	Slope (β)
$\ln(DH)$	0.382041	0.815684	6.524	0.689	0.646596	-1.1174	0.8066
$\ln(D^2H)$	0.624536	0.808669	10.119	1.136	0.63298	-0.7326	0.4817
$\ln(D^2HW)$	0.629540	0.850021	9.605	1.089	0.6937	-0.9025	0.5250

Linear Regression Models

The regression models were all good fit for their respective variables (Table 1; Figure 1). The intercept and slope for the regression models were -1.1174 and 0.8066 for In (DH), -0.7326 and 0.4817 for In(D^2H), and -0.9025 and 0.5250 for In(D^2HW) (Figure 1). The R-squared values were 0.646596, 0.63298, and 0.6937 for In(DH), In(D^2H), and In(D^2HW) respectively (Table 1).

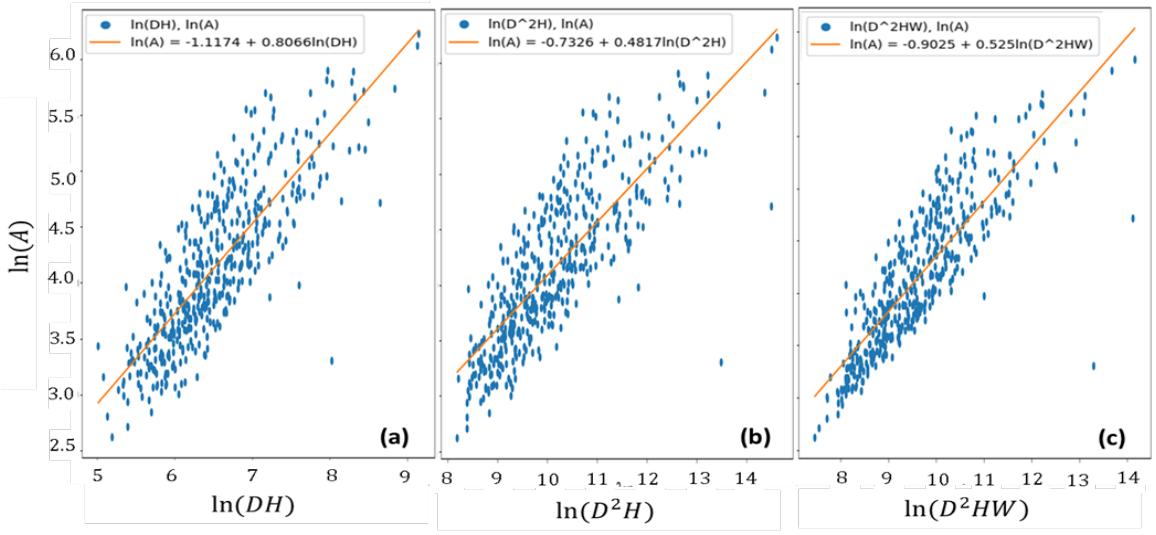

Figure 1: Scatter plot of the variables under Study with Regression Line

Artificial Neural Networks

The input variables used in the linear regression modelling were slightly altered for the ANNs to be able to accommodate them. From the laws of logarithm, the input variables in equations 6, 7, and 8 can each be rewritten as a linear combination of the natural logarithm of the individual allometric measurements that make up the variable.

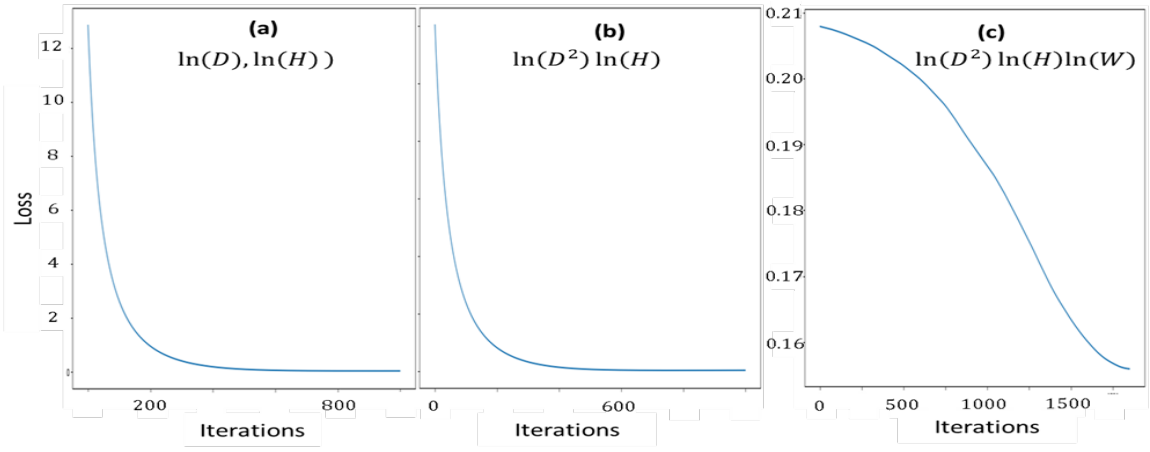

Figure 2: Graphs Training Loss against number of Iterations for each Neural Network

$$\ln(DH) = \ln(D) + \ln(DH) \tag{25}$$

$$\ln(D^2H) = \ln(D^2) + \ln(H) \tag{26}$$

$$\ln(D^2HW) = \ln(D^2) + \ln(H) + \ln(D^2HW) \tag{27}$$

The values on the right-hand side of equations 25, 26, and 27 make up the input variables for the respective ANNs under study (Table 2, Table 3, and Table 4). The first and second ANNs (Figure 3, Figure 4) showed a rapid decline rate of training loss with fewer iterations, while the third ANN (Figure 5) showed a less steep decline with more iterations (Figure 2).

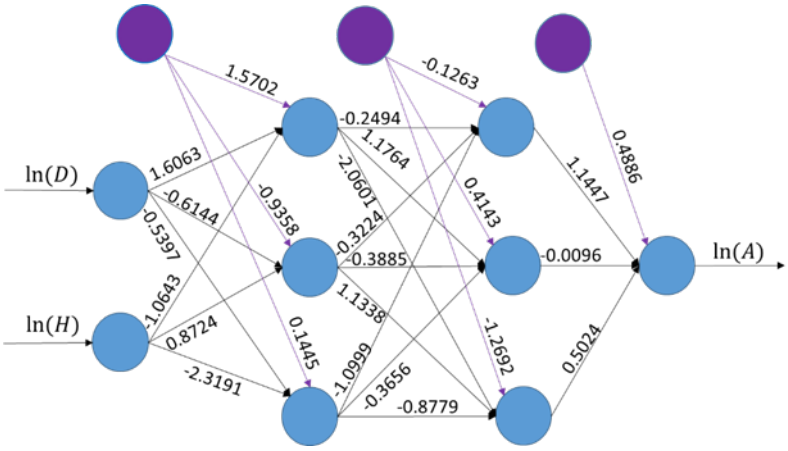

Figure 3: Architecture of the First Neural Network

Table 2: Weights and Biases of the First Neural Network

Layer 1	**Bias**	ln (D)	ln (H)	
Node 1	1.5702	1.6064	-1.0643	
Node 2	-0.9358	-0.6143	0.8724	
Node 3	0.1445	-0.5397	-2.3192	
Layer 2	**Bias**	**Layer 1**	**Layer 1**	**Layer 1**
		Node 1	**Node 2**	**Node 3**
Node 1	-0.1263	-0.2494	-0.3224	-1.0999
Node 2	0.4143	1.1764	-0.3885	-0.3656
Node 3	-1.2692	-2.0601	1.1338	-0.8779
Layer 3	**Bias**	**Layer 2**	**Layer 2**	**Layer 2**
ln (A)	0.4886	1.1447	-0.0096	0.5025

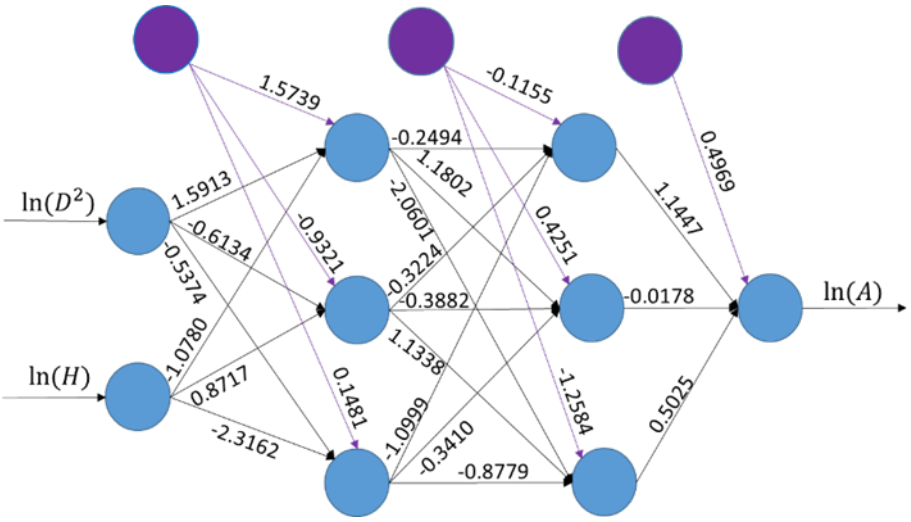

Figure 4: Architecture of the Second Neural Network

Table 3: Weights and Biases of the Second Neural Network

Layer 1	**Bias**	$\ln(D^2)$	$\ln(H)$	
Node 1	1.5739	1.5913	-1.0780	
Node 2	-0.9321	-0.6134	0.8718	
Node 3	0.1481	-0.5374	-2.3163	
Layer 2	**Bias**	**Layer 1**	**Layer 1**	**Layer 1**
		Node 1	**Node 2**	**Node 3**
Node 1	-0.1155	-0.2494	-0.3224	-1.0999
Node 2	0.4251	1.1802	-0.3882	-0.3410
Node 3	-1.2584	-2.0601	1.1338	-0.8778
Layer 3	**Bias**	**Layer 2**	**Layer 2**	**Layer 2**
		Node 1	**Node 2**	**Node 3**
$\ln(A)$	0.4969	1.1447	-0.0178	0.5025

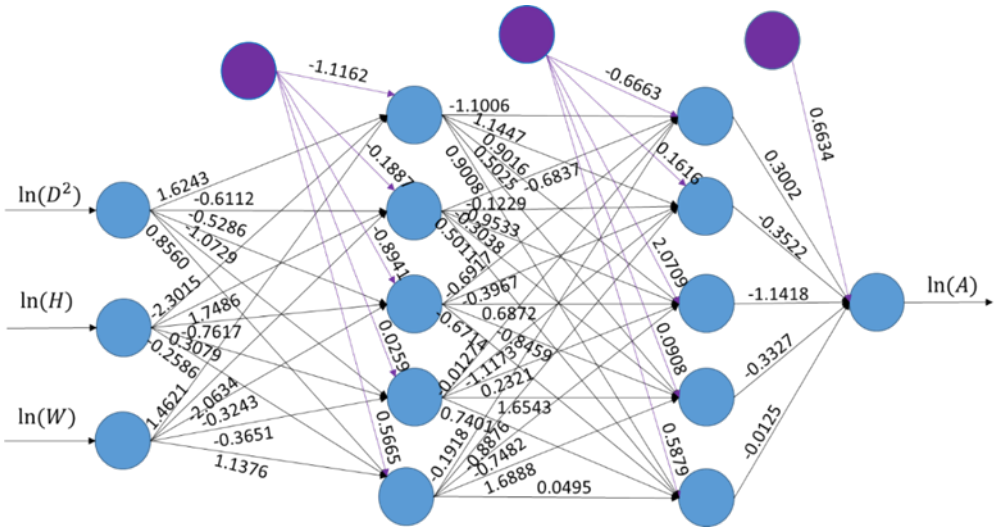

Figure 5: Architecture of the Third Neural Network

Table 4: Weights and Biases of the Third Neural Network

Layer 1	**Bias**	$\ln(D^2)$	$\ln(H)$	$\ln(W)$		
Node 1	-1.1162	1.6244	-2.3015	1.4621		
Node 2	-0.1887	-0.6113	1.7486	-2.0634		
Node 3	-0.8941	-0.5287	-0.7617	-0.3244		
Node 4	0.0260	-1.0730	0.3080	-0.3651		
Node 5	0.5666	0.8560	-0.2586	1.1377		
Layer 2	**Bias**	**Layer 1 Node 1**	**Layer 1 Node 2**	**Layer 1 Node 3**	**Layer 1 Node 4**	**Layer 1 Node 5**
Node 1	-0.6663	-1.1006	-0.6837	-0.6917	-0.0127	-0.1918
Node 2	0.1616	1.1447	-0.1229	-0.3968	-1.1173	-0.8876
Node 3	2.0709	0.9016	-0.9533	-0.6872	0.2321	-0.7482
Node 4	0.0909	0.5025	-0.3038	-0.8459	1.6543	1.6888
Node 5	0.5879	0.9009	0.5011	-0.6714	0.7401	0.0495
Layer 3	**Bias**	**Layer 2 Node 1**	**Layer 2 Node 2**	**Layer 2 Node 3**	**Layer 2 Node 4**	**Layer 2 Node 5**
$\ln(A)$	0.6634	0.3002	-0.3523	-1.1418	-0.3327	-0.0125

Comparative Accuracy Analysis

The training RMSE's for the linear regression models were 0.3967, 0.4043, and 0.3693 while the test RMSE's were 0.3761, 0.3784, and 0.3060 (Table 5).

Table 5: Model Accuracy Measurement

Model Type	Explanatory Variables	RMSE	
		Training	Test
Linear Regression	$\ln(DH)$	0.3967	0.3761
	$\ln(D^2H)$	0.4043	0.3784
	$\ln(D^2HW)$	0.3693	0.3060
Neural Network	$\ln(D)$, $\ln(H)$	0.1997	0.2199
	$\ln(D^2)$, $\ln(H)$	0.2113	0.2284
	$\ln(D^2)$, $\ln(H)$, $\ln(W)$	0.3949	0.3812

Maximum loss for each neural network was 12.8393, 12.0371, and 0.2078, while minimum loss were 0.0391; 0.0408; and 0.1559. Accuracy was measured using Root Mean Squared Error (RMSE) with the training RMSE' as 0.1997, 0.2113 and 0.3949, while test RMSE's was 0.2199, 0.2284, and 0.3812 for each neural network.

This study investigated the impact of applying ANNs with different input variables and different architectures to estimate AGB using allometric data from tropical forests in Southwestern Nigeria. The study also compared the result of ANNs with linear regression and found out that the ANN models performed better than the linear regression models. Two things were a factor in the accuracy of the models. The first was the number of input variables. The models with more input variables performed better than other models within the same category. In conclusion, the architecture of the neural network, and the nature and number of the input variables are significant factors in the accuracy of the ANN models. Also, ANNs are a valuable way of modeling AGBs.

REFERENCES

Ali A, Xu MS, Zhao YT, Zhang QQ, Zhou LL, Yang XD, Yan ER 2015. Allometric biomass equations for shrub and small tree species in subtropical China. *Silva Fennica* 49:1–10. https://doi.org/10.14214/sf.1275

Baccini A, Walker W, Carvalho L, Farina M, Sulla-Menashe D, Houghton RA 2017. Tropical forests are a net carbon source based on aboveground measurements of gain and loss. *Science* 358:230–234. https://doi.org/10. 1126/science.aam5962

Bernacchi, C.J., Coleman, J.S., Bazzaz, F.A., McConnaughay, K.D.M. 2000. Bio-

mass allocation in old-field annual species grown in elevated CO2 environments: no evidence for optimal partitioning. *Global Change Biology* 6(7): 855–863.

Chave J, Réjou-Méchain M, Búrquez A, Chidumayo E, Colgan MS, Delitti WB, Duque A, Eid T, Fearnside PM, Goodman RC, Henry M, Martinez-Yrizar A, Mugasha WA, Muller-Landau HC, Mencuccini M, Nelson BW, Ngomanda A, Nogueira EM, Ortiz-Malavassi E, Pelissier R, Ploton P, Ryan CM, Saldarriaga JG, Vieilledent G 2014. Improved allometric models to estimate the aboveground biomass of tropical trees. *Global Change Biology* 20:3177–3190. https://doi.org/10.1111/gcb.12629

Chave, J., Réjou-Méchain, M., Búrquez, A., Chidumayo, E., Colgan, M. S., Delitti, W. B. C., Vieilledent, G. 2014. Improved allometric models to estimate the aboveground biomass of tropical trees. *Global Change Biology* 20(10): 3177–3190. http://doi.org/10.1111/gcb.12629

Elzinga, C., Shearer, R. C., & Elzinga, G. 2005. Observer Variation in Tree Diameter Measurements. *Western Journal of Applied Forestry* 20(2): 134–137, https://doi.org/10.1093/wjaf/20.2.134

Fukushima, K. 1980. Neocognitron: A Self-organizing Neural Network Model for a Mechanism of Pattern Recognition Unaffected by Shift in Position. *Biological Cybernetics* 36: 193 – 202.

Hunter, J. D. 2007. Matplotlib: A 2D graphics environment. *Computing in Science & Engineering* 9(3), 90–95. Doi:10.1109/MCSE.2007.55

Kumar L, Sinha P, Taylor S, Alqurashi AF 2015. Review of the use of remote sensing for biomass estimation to support renewable energy generation. *Journal of Applied Remote Sensing* 9:976-996

McKinney, W., & others. 2010. Data structures for statistical computing in python. In Proceedings of the 9th Python in Science Conference. 445, 51–56.

Nair, V., and Hilton, G. E. 2010. Rectified Linear Units Improve Restricted Boltzmann Machines. In *Proceedings of the 27th International Conference on Machine Learning*, Haifa, Israel, 2010.

Oliphant, T. E. 2006. A guide to NumPy (Vol. 1). Trelgol Publishing USA.

Pan Y, Birdsey RA, Fang J, Houghton R, Kauppi PE, Kurz WA, Phillips OL, Shvidenko A, Lewis SL, Canadell JG, Ciais P, Jackson RB, Pacala SW, McGuire AD, Piao SL, Rautiainen A, Sitch S, Hayes D 2011. A large and persistent carbon sink in the world's forests. *Science*, 333:988–993. https://doi.org/10.1126/science.1201609

Paul KI, Roxburgh SH, Chave J, England JR, Zerihun A, Specht A, Lewis T, Bennett LT, Baker TG, Adams MA, Huxtable D, Montagu KD, Falster DS, Feller M, Sochacki S, Ritson P, Bastin G, Bartle J, Inildy D, Hobbs T, Armour JL, Waterworth R, Stewart HTL, Jonsonf J, Forrester DI, Applegate G, Mendhan D, Bradford M, O'Grady A, Green D, Sudmeyer R, Rance SJ, Turner J, Barton C, Wenk EH, Grove T, Attiwill PM, Pinkard E, Butler D, Brooksbank K, Spencer B, Snowdon P, O'Brien N, Battaglia M, Cameron DM, Hamilton S, Mcauthur G,

Sinclair A 2015. Testing the generality of above-ground biomass allometry across plant functional types at the continent scale. *Global Change Biology* 22:2106–2124

Pedregosa, F., Varoquaux, G., Gramfort, A., Michel, V., Thirion, B., Grisel, O., Blondel, M., Prettenhofer, P., Weiss, R., Dubourg, V., Vanderplas, J., Passos, A., Cournapeau, D., Brucher, M., Perrot, M., and Duchesnay, E. 2011. Scikit-learn: Machine Learning in Python. *Journal of Machine Learning Research* 12: 2825-2830.

Picard, N., Rutishauser, E., Ploton, P., Ngomanda, A., & Henry, M. 2015. Forest Ecology and Management Should tree biomass allometry be restricted to power models ? *Forest Ecology and Management*, 353, 156–163. https://doi.org/10.1016/j.foreco.2015.05.035

Rodríguez-Soalleiro R, Eimil-Fraga C, Gómez-García E, García-Villabrille JD, Rojo- Alboreca A, Muñoz F, Oliveira N, Sixto H, Pérez-Cruzado C 2018. Exploring the factors affecting carbon and nutrient concentrations in tree biomass components in natural forests, forest plantations and short rotation forestry. *Forest Ecosystems*, 5:35. https://doi.org/10.1186/s40663-018-0154-y

Schmidhuber, J. 2014. Deep Learning in Neural Networks: An Overview. Technical Report IDSIA-03-14 / arXiv:1404.7828 v4 [cs.NE].

Sileshi, G.W. 2014. A critical review of forest biomass estimation models, common mistakes and corrective measures. *Forest Ecology and Management* 329, 237–254.

Stevens, C.F. 2009. Darwin and Huxley revisited: the origin of allometry. Journal of Biology, 8 (2), PMC2687774.

Van Rossum, G., Drake, F. L. 2009. Python 3 Reference Manual. Scotts Valley, CA: CreateSpace.

Virtanen, P., Gommers, R., Oliphant, T. E., Haberland, M., Reddy, T., Cournapeau, D., Burovski, E., Peterson, P., Weckesser, W., Bright, J., van der Walt, S. J., Brett, M., Wilson, J., Jarrod Millman, K., Mayorov, N., Nelson, A. R.–J. Jones, E., Kern, R., Larson, E., Carey, C. J., Polat, I., Feng, Y., Moore, E. W., VanderPlas, J., Laxalde, D., Perktold, J., Cimrman, R., Henriksen, I., Quintero, E. –A. Harris, C. R., Archibald, A. M., Ribeiro, A.H., Pedregosa, F., van Mulbregt, Paul and SciPy 1.0 Contributors. 2020. SciPy 1.0: Fundamental Algorithms for Scientific Computing in Python. *Nature Methods* 17, 261 – 272. Doi: 10.1038/s41592-019-0686-2

(Manuscript received: 11th October, 2022; accepted: 22nd December, 2022).